RECENT THEORETICAL RESULTS FOR ELECTROMAGNETICALLY-INDUCED ULTRAPERIPHERAL REACTIONS OF HEAVY IONS*

A. Szczurek

Institute of Nuclear Physics Polish Academy of Sciences
Radzikowskiego 152, 31-342 Kraków, Poland
and
Faculty of Mathematics and Natural Sciences
University of Rzeszów
Pigonia 1, 35-310 Rzeszów Poland

(Received December 20, 2018)

We briefly review our works on ultraperipheral heavy-ion collisions. We discuss both $\gamma\gamma$ and rescattering of hadronic photon fluctuation induced by one nucleus in the collision partner. Production of one and two leptonic and pionic, and $p\bar{p}$ pairs is discussed as an example of photon–photon processes. The production of single vector mesons (ρ^0 or J/ψ) is an example of the second category. The double-scattering mechanisms of two ρ^0 meson production is discussed in addition.

DOI:10.5506/APhysPolBSupp.12.323

1. Introduction

The ultraperipheral collisions is a class of processes that were studied experimentally only recently at RHIC and the LHC. The processes can be viewed as a scattering of two clouds of photons or a process of scattering of a photon (or photon hadronic fluctuations) emitted by one nucleus on the second colliding nucleus. In general, one is interested rather in processes with small particle multiplicity which automatically means that the impact parameter is greater than the sum of the radii of colliding nuclei. Some of such processes were suggested long ago [1]. Only recently, some experimental results were presented. In the following, we will present some results. In addition, we will show some other processes that could be also studied at the LHC.

* Presented at the XIII Workshop on Particle Correlations and Femtoscopy, Kraków, Poland, May 22–26, 2018.

A schematic view of the photon-induced processes is shown in Fig. 1 and the situation in the impact parameter space is illustrated in Fig. 2. When calculating the cross section in the equivalent photon approximation in the impact parameter space, ultraperipheral collisions mean that the two circles, representing heavy ions, do not overlap ($b > R_A + R_B$) [1]. It does not mean, however, that the processes of photoproduction disapear in such a case. In this case, they may also contribute and compete with other procesess characteristic for standard ($b < R_A + R_B$) heavy-ion collisions. The situation/physics then strongly depends on the reaction.

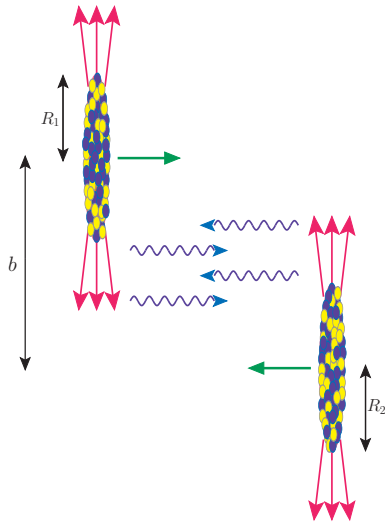

Fig. 1. A schematic view of the $\gamma\gamma$ induced processes.

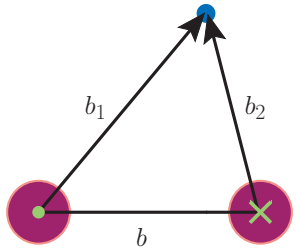

Fig. 2. The situation in the impact parameter space.

Our detailed studies were presented in Refs. [2–16]. In this paper, we discuss different processes except light-by-light processes that were discussed in [17]. Here, we only sketch some selected results.

2. A brief review of our results for UPC

We start presentation of our results for dilepton production. In Fig. 3, we present our results for dielectron invariant mass together with the ALICE experimental data [18]. Good agreement is achieved without free parameters.

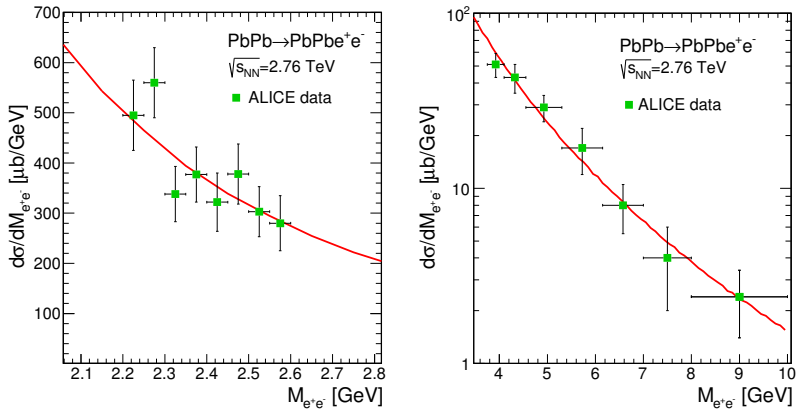

Fig. 3. Dielectron invariant mass for the $\mathrm{Pb}\,\mathrm{Pb} \to \mathrm{Pb}\,\mathrm{Pb}\,e^+e^-$ for the ALICE experimental cuts [18].

In Fig. 4, we present our results together with the ATLAS data [19] for the $\mathrm{Pb}+\mathrm{Pb} \to \mathrm{Pb}+\mathrm{Pb}+\mu^+ + \mu^-$ reaction. Experimental cuts were included in our calculations. In contrast to the $\mathrm{Pb}\,\mathrm{Pb} \to \mathrm{Pb}\,\mathrm{Pb}\,e^+e^-$ reaction, the agreement here is much worse.

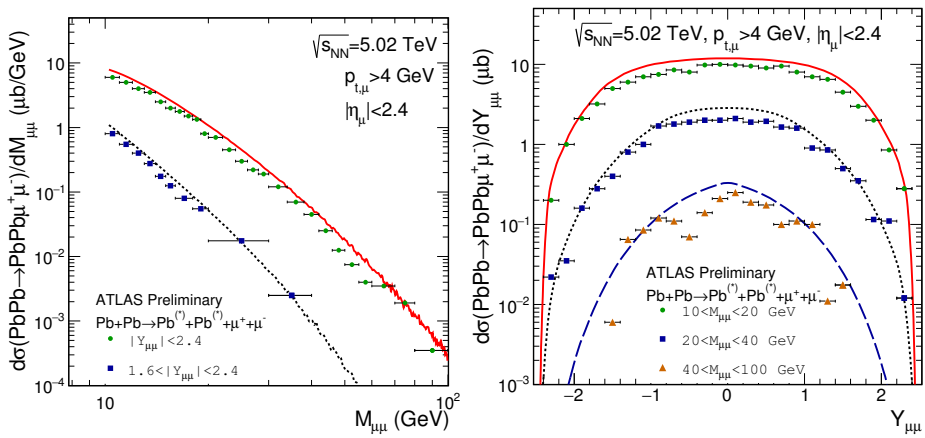

Fig. 4. Cross section for dimuon production in UPC of Pb+Pb together with the ATLAS experimental data [19].

Let us now briefly discuss production of charged pion pairs. In Fig. 5, we demonstrate how well our multicomponent model [5] describes the elementary cross sections for $\gamma\gamma \to \pi^+\pi^-$ and $\gamma\gamma \to \pi^0\pi^0$ measured in detail by different experiments [5]. These elementary cross sections can be used in calculation of the cross section for nuclear processes $AA \to AA\pi\pi$.

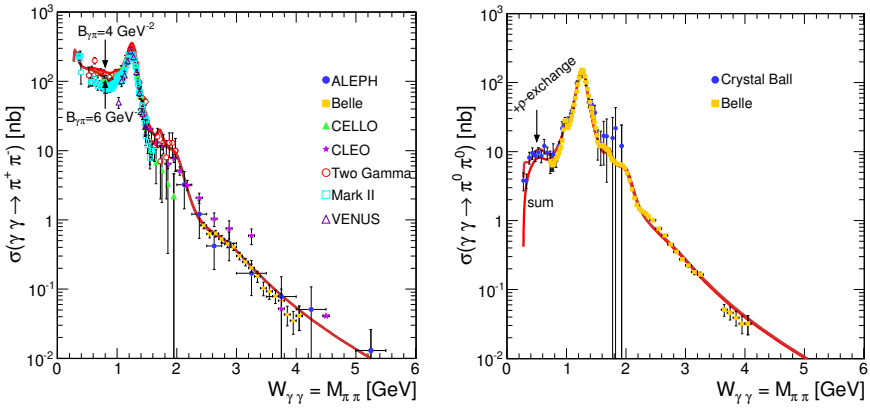

Fig. 5. Energy dependence of the elementary cross sections for $\gamma\gamma \to \pi\pi$ reactions.

There is a strong competition in the $\pi^+\pi^-$ channel of coherent ρ^0 meson production (see Fig. 6) which decays into a $\pi^+\pi^-$ pair. The main mechanism is photon fluctuation into virtual ρ^0 meson and its multiple rescattering in the collision partner. In Fig. 7, we show invariant mass distribution of the $\pi^+\pi^-$ system. Both ρ^0 contribution with effective inclusion of the photoproduction continum, called sometimes Söding mechanism, and the $\gamma\gamma$ mechanism were considered. The $\gamma\gamma$ mechanism becomes sizeable in the region of the $f_2(1270)$ dipion resonance and its presence improves agreement with the ALICE experimental data [20].

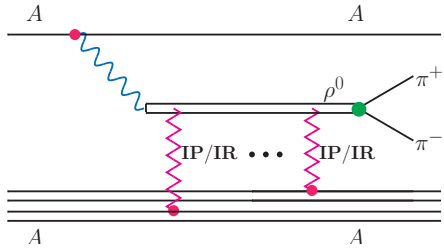

Fig. 6. Mechanism of coherent ρ^0 production.

The cross section for coherent single ρ^0 production is very large. Therefore, one could consider also double-scattering cross section for production of $\rho^0\rho^0$ pairs. The underlying mechanisms are sketched in Fig. 8.

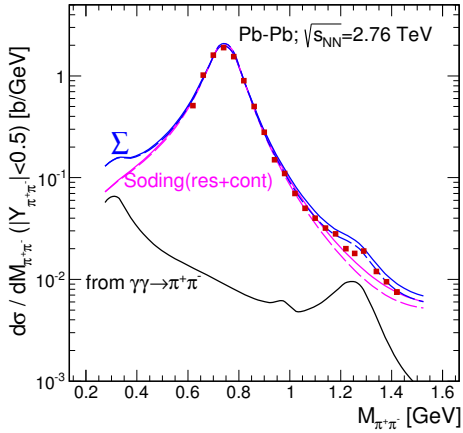

Fig. 7. Dipion invariant mass together with the ALICE experimental data [20]. The $\rho^0 \to \pi^+\pi^-$ and $\gamma\gamma \to \pi^+\pi^-$ contributions are shown separately.

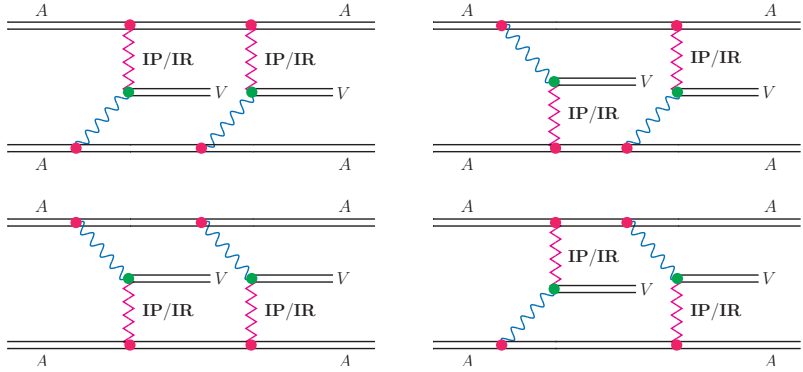

Fig. 8. The mechanisms of double ρ^0 production.

In Fig. 9, we show distribution in four-pion invariant mass for $\sqrt{s_{NN}} =$ 200 GeV together with the STAR data [21]. We show the $\gamma\gamma \to \rho^0\rho^0$ and double-scattering contributions. Clearly, the double scattering contribution is larger than the $\gamma\gamma$ one but insufficient to understand the STAR data [21]. Is the disagreement due to coherent production of ρ' or ρ'' mesons? This is not clear at the moment and requires further studies in the future.

In Fig. 10, we show our predictions for four-pion invariant mass, including only double-scattering mechanism for $\sqrt{s_{NN}} = 2.76$ TeV. The resulting distribution strongly depends on the range of rapidity. A longer range is preferred when one wants to enhance the double-scattering contribution.

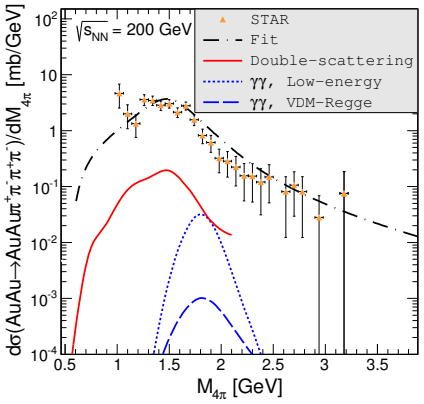

Fig. 9. Color online)Four-pion invariant mass distribution calculated by us together with the STAR experimental data [21]. The contribution of the double scattering mechanism is shown by the solid blue line. In addition, we show contribution of single scattering based on $\gamma\gamma \to \rho^0\rho^0$ subprocess subdivided into two subcontributions described in [4].

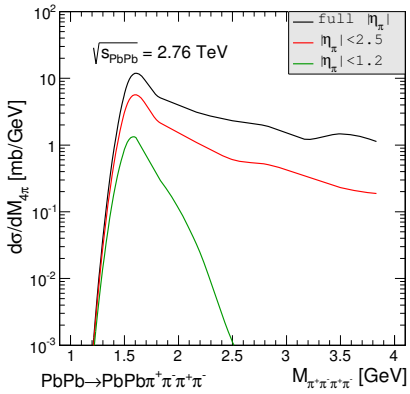

Fig. 10. Four-pion invariant mass at the LHC for different ranges of pion pseudorapidity.

Another interesting process is $AA \to AAp\bar{p}$. The continuum subprocess is shown, for example, in Fig. 11. In our studies, we included also some resonances [11]. In Fig. 12, we show our predictions for $M_{p\bar{p}}$ and rapidity distributions for $\mathrm{Pb\,Pb} \to \mathrm{Pb\,Pb}\,p\bar{p}$ process at $\sqrt{s_{NN}} = 5.02$ TeV. Predicted cross sections for $\mathrm{Pb\,Pb} \to \mathrm{Pb\,Pb}\,p\bar{p}$ for different experimental cuts are given in Table I.

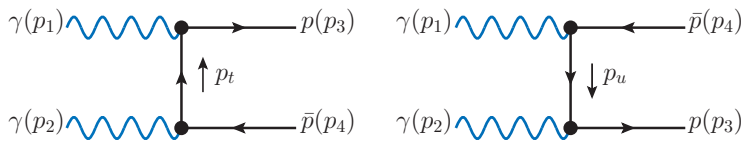

Fig. 11. Elementary processes $\gamma\gamma \to p\bar{p}$ responsible for production of $p\bar{p}$ pairs in UPC of heavy ions.

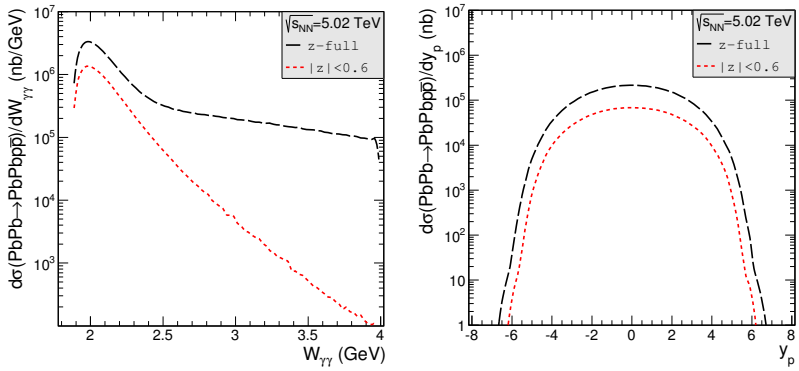

Fig. 12. Examples of differential cross sections for the $\mathrm{Pb\,Pb} \to \mathrm{Pb\,Pb}\,p\bar{p}$ reaction.

TABLE I

Experiment	Cuts	σ [μb]
ALICE	$p_{\mathrm{t},p} > 0.2$ GeV, $\lvert y_p\rvert < 0.9$	100
ATLAS	$p_{\mathrm{t},p} > 0.5$ GeV, $\lvert y_p\rvert < 2.5$	160
CMS	$p_{\mathrm{t},p} > 0.2$ GeV, $\lvert y_p\rvert < 2.5$	500
LHCb	$p_{\mathrm{t},p} > 0.2$ GeV, $2 < y_p < 4.5$	104

Double scattering UPC are possible also for production of two lepton pairs as shown in Fig. 13. The cross section integrated over phase space is shown in Fig. 14 for two different cuts on lepton transverse momenta (the same for each lepton).

The number of counts for integrated luminosity $L_{\mathrm{int}} = 1\ \mathrm{nb}^{-1}$ is given in Table II. The table shows that some measurements of four leptons are possible. Certainly, such a test of our predictions of double scattering mechanism would be new and valuable.

Many of the processes discussed here survive also to the situation when the nuclei collide and when centrality of the collision can be determined. A first example was discussed for photoproduction of J/ψ quarkonium in [12].

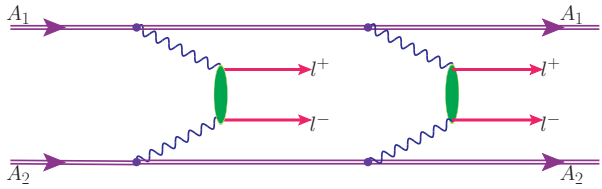

Fig. 13. Double scattering production mechanism of two lepton pairs.

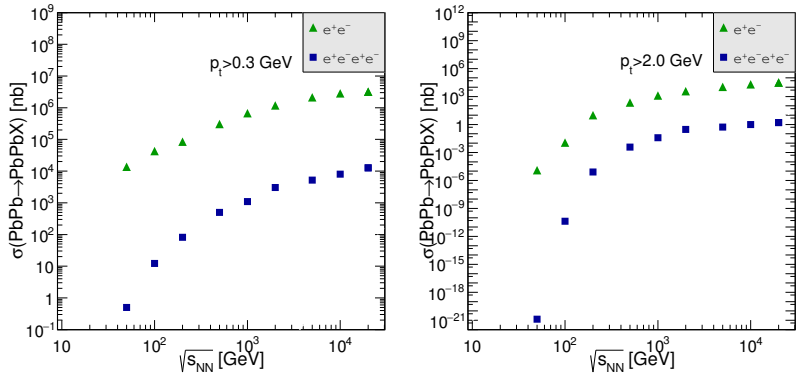

Fig. 14. Phase-space integrated cross section for $e^+e^-e^+e^-$ and e^+e^- production for two different cuts on lepton transverse momenta.

TABLE II

(4μ), $\sqrt{s_{NN}} = 5.02$ TeV		$(4e)$, $\sqrt{s_{NN}} = 5.5$ TeV	
Experimental cuts	N	Experimental cuts	N
$\lvert y_i\rvert < 2.5$, $p_t > 0.5$ GeV	815	$\lvert y_i\rvert < 2.5$, $p_t > 0.5$ GeV	235
$\lvert y_i\rvert < 2.5$, $p_t > 1.0$ GeV	53	$\lvert y_i\rvert < 2.5$, $p_t > 1.0$ GeV	10
$\lvert y_i\rvert < 0.9$, $p_t > 0.5$ GeV	31	$\lvert y_i\rvert < 1.0$, $p_t > 0.2$ GeV	649
$\lvert y_i\rvert < 0.9$, $p_t > 1.0$ GeV	2	$\lvert y_i\rvert < 1.0$, $p_t > 1.0$ GeV	1
$\lvert y_i\rvert < 2.4$, $p_t > 4.0$ GeV	$\ll 1$		

In Fig. 15, we show the cross section for different bins of centrality. Rather good description of the data was achieved by imposing special conditions on photon fluxes [12].

Another example is the $AA \to e^+e^-$ peripheral and semicentral nucleus–nucleus collisions for small dilepton transverse momenta discussed very recently [16]. The photoproduction mechanism is particularly important for small dielectron transverse momenta and not too small energies where it competes with thermal dielectron production.

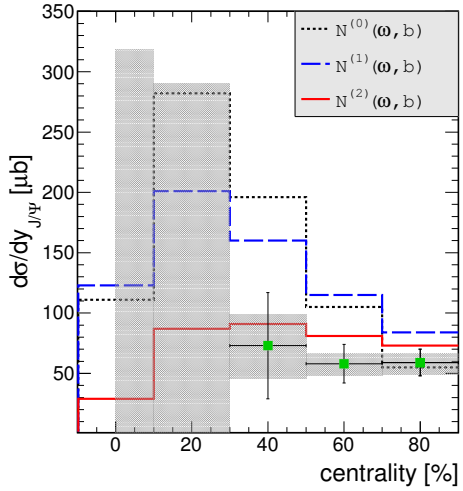

Fig. 15. Dependence of the cross section for creation of the J/ψ meson as a function of meson centrality together with the ALICE experimental data [22].

This work was supported by the National Science Centre, Poland (NCN), grant number 2014/15/B/ST2/02528.

REFERENCES

[1] V.M. Budnev, I.F. Ginzburg, G.V. Meledin, V.G. Serbo, *Phys. Rep.* **15**, 4 (1975); C.A. Bertulani, G. Baur, *Phys. Rep.* **163**, 29 (1988); G. Baur *et al.*, *Phys. Rep.* **364**, 359 (2002); A.J. Baltz *et al.*, *Phys. Rep.* **458**, 1 (2008).

[2] M. Kłusek-Gawenda, A. Szczurek, *Phys. Rev. C* **82**, 014904 (2010).

[3] M. Kłusek-Gawenda, A. Szczurek, M. Machado, V. Serbo, *Phys. Rev. C* **83**, 024903 (2011).

[4] M. Kłusek, W. Schäfer, A. Szczurek, *Phys. Lett. B* **674**, 92 (2009).

[5] M. Kłusek-Gawenda, A. Szczurek, *Phys. Rev. C* **87**, 054908 (2013).

[6] M. Kłusek-Gawenda, A. Szczurek, *Phys. Lett. B* **700**, 322 (2011).

[7] S. Baranov *et al.*, *Eur. Phys. J. C* **73**, 2335 (2013).

[8] M. Kłusek-Gawenda, A. Szczurek, *Phys. Rev. C* **89**, 024912 (2014).

[9] M. Kłusek-Gawenda, P. Lebiedowicz, A. Szczurek, *Phys. Rev. C* **93**, 044907 (2016).

[10] M. Kłusek-Gawenda, W. Schäfer, A. Szczurek, *Phys. Lett. B* **761**, 399 (2016).

[11] M. Kłusek-Gawenda, P. Lebiedowicz, O. Nachtmann, A. Szczurek, *Phys. Rev. D* **96**, 094029 (2017).

[12] M. Kłusek-Gawenda, A. Szczurek, *Phys. Lett. B* **763**, 416 (2016).

[13] A. Hameren, M. Kłusek-Gawenda, A. Szczurek, *Phys. Lett. B* **776**, 84 (2018).
[14] M. Kłusek-Gawenda, A. Szczurek, *Phys. Rev. C* **93**, 044912 (2016).
[15] M. Kłusek-Gawenda, M. Ciemała, W. Schäfer, A. Szczurek, *Phys. Rev. C* **89**, 054907 (2014).
[16] M. Kłusek-Gawenda, R. Rapp, W. Schäfer, A. Szczurek, *Phys. Lett. B* **790**, 339 (2019) [arXiv:1809.07049 [nucl-th]].
[17] M. Kłusek-Gawenda, *Acta Phys. Pol. B Proc. Suppl.* **12**, 333 (2019), this issue.
[18] E. Abbas *et al.* [ALICE Collaboration], *Eur. Phys. J. C* **73**, 2617 (2013).
[19] ATLAS Collaboration, ATLAS-CONF-2016-025.
[20] J. Adam *et al.* [ALICE Collaboration], *J. High Energy Phys.* **1509**, 095 (2015).
[21] B.I. Abelev *et al.* [STAR Collaboration], *Phys. Rev. C* **81**, 044901 (2010).
[22] J. Adam *et al.* [ALICE Collaboration], *Phys. Rev. Lett.* **116**, 222301 (2016).